Supporting Information for

Resolving the Growth of 3D Colloidal Nanoparticle Superlattices by Real-time Small Angle X-ray Scattering

Chenguang Lu, Austin J. Akey, Clayton J. Dahlman, Datong Zhang and Irving P. Herman
Department of Applied Physics and Applied Mathematics
Columbia University, New York, NY 10027, U.S.A.

1) Additional Experimental Details

To synthesize iron oxide nanoparticles, a mixture of 15 mL octadecene and 1.8 mL oleic acid was degassed at 100°C for 1 hr, followed by injection of 0.3 mL iron pentacarbonyl. The mixture was heated to 300°C and held at that temperature for 1 h. This product was exposed to air for ~30 min (to transform the NPs to magnetite), and was then washed by ethanol three times and dispersed in toluene. This procedure produces NPs of diameter ~11 nm, which was varied by adjusting the amount of oleic acid. Particle sizes were determined using SAXS, as described below.

The vacuum chamber (Fig. S1), placed on an elevated stage, had two Kapton® windows for the incoming and scattered x-ray beams, and valves from the nitrogen inlet and to the vacuum pump to control pressure. It was sealed ~60 s after drop casting and the first x-ray irradiation started ~26 s later. During solvent evaporation, SAXS data were accumulated on a given spot for 3 s, before the sample was laterally moved to a fresh spot on the drying film for another cycle of data collection starting 60 s later, until no more changes in the SAXS patterns were seen and the film was presumably dry.

There was evidence of modifications to the film microstructure (by optical and electron microscopy) and nanostructure (by SAXS) when the sample was not moved during irradiation cycles and when the sample was moved during drying but the irradiation durations were longer (~15 s) than used here. Details about these modifications can be found in Ref. 1.

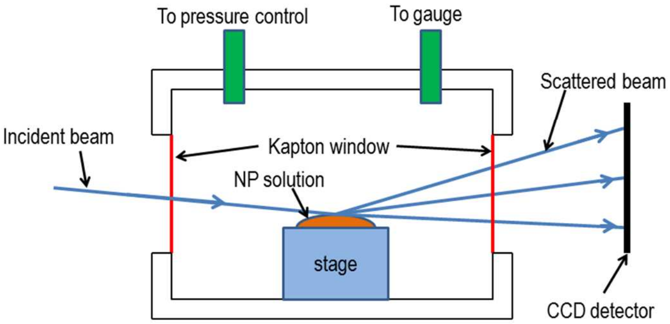

Figure S1. Schematic of the chamber used for NP superlattice growth and *in situ* SAXS analysis. The chamber pressure can be tuned from 1 to 760 Torr.

2) Additional Experimental Information

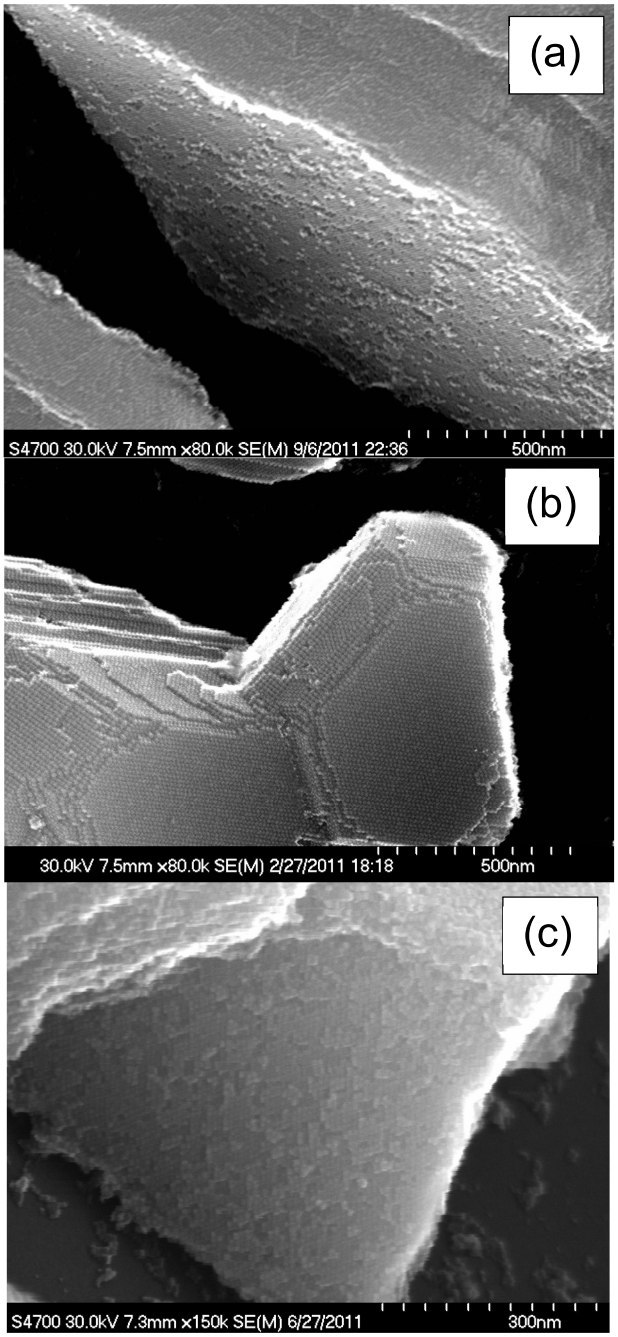

Figure S2. SEM images of SNSLs made from (a) 10.6 nm, (b) 12.4 nm, and (c) 5.9 nm diameter iron oxide NPs.

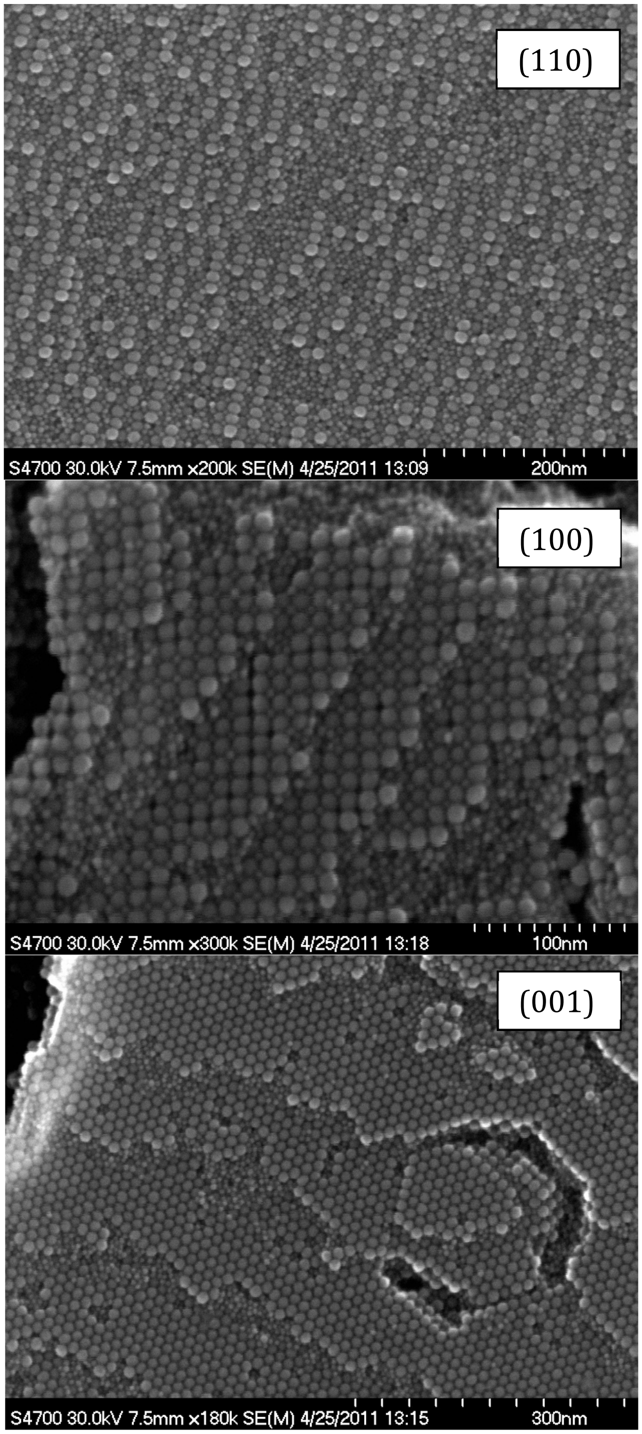

Figure S3. SEM images of BNSLs, showing the (110), (100), and (001) facets of a BNSL formed using 12.4 and 5.9 nm diameter iron oxide NPs.

The sizes of the NP cores were determined by fitting their SAXS form factors [*P(q,R)*] to:

$$P(q,R) = v^2 \left[\frac{\sin(qR) - (qR)\cos(qR)}{(qR)^3}\right]^2 \qquad (S1)$$

where *q* is the scattering wave vector, *R* is the nanoparticle core radius, and *v* is the nanoparticle volume, and assuming a Gaussian size distribution with a standard deviation in the normalized diameter given in Table S1.

Average radius (*R*, nm)	7.65	6.9	6.2	5.3	2.95
Average diameter (nm)	15.3	13.8	12.4	10.6	5.9
Standard deviation	3.92%	8.7%	4.03%	5.66%	10.2%

Table S1. Dispersion in particle size.

The method for indexing SLs is illustrated in Figure S4.

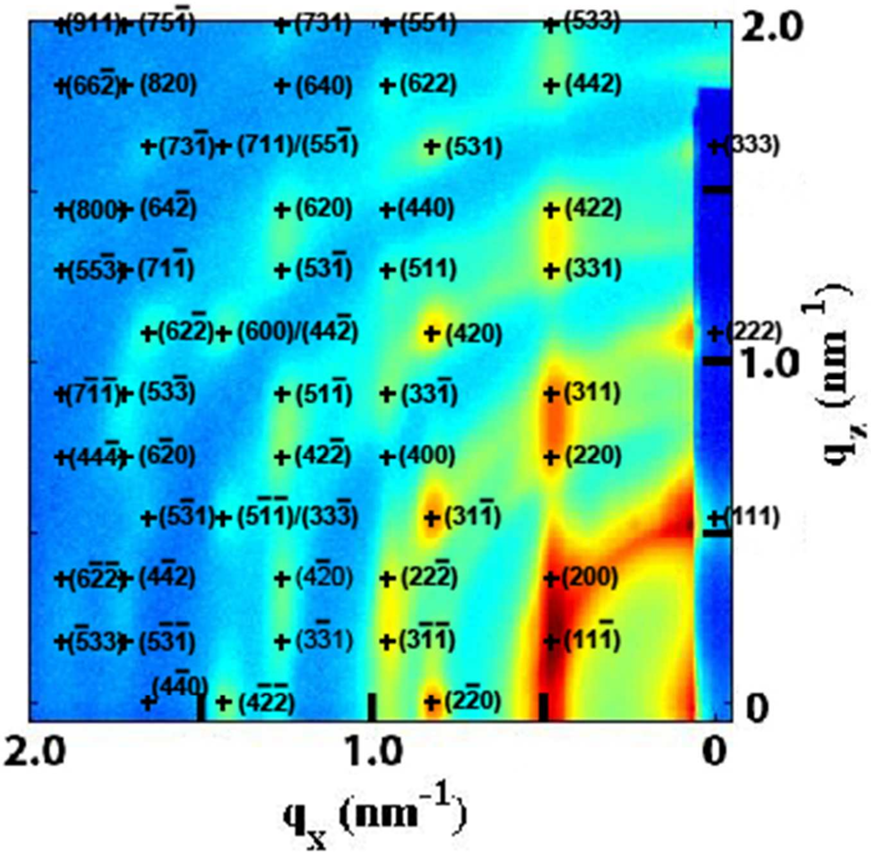

Figure S4. Method for indexing *fcc* SNSLs. The positions of the generated diffraction spots were adjusted to the SAXS pattern for this 13.8 nm iron oxide NP SNSL to calculate the SNSL lattice constants and NP nearest neighbor distances.

Movie S1 shows the evolution of the SAXS pattern during the formation of 13.8 nm iron oxide NP SNSL, as seen in the Figure 2a-c snapshots in the main text. Movie S2 depicts the evolution of the nearest neighbor interaction potentials during solvent evaporation, as seen in the Figure 3a-c snapshots in the main text. Movie S3 shows the evolution of the SAXS pattern during the formation of the BNSL described the Figure 4a-c snapshots in the main text.

3) Inter-NP Potential Modeling

The potential profile modeling[2] included the Van der Waals force between NP cores (Φ_{osm}), osmotic pressure from the mixing of solvent and ligand (Φ_{osm}), and elastic repulsion between approaching NP ligands (Φ_{elas}). The sum of the above was compared with Brownian motion energy, 3/2 k_BT per NP, which was used to assess the favorability of SNSL formation.

The potential profile modeling used the following potentials:

$$\Phi_{VdW} = -\frac{A}{6}\left[\frac{2R^2}{h^2 + 4Rh} + \frac{2R^2}{h^2 + 4Rh + 4R^2} + \ln\left(\frac{h^2 + 4Rh}{h^2 + 4Rh + 4R^2}\right)\right] \tag{S2}$$

$$\Phi_{osm} = \begin{cases} \dfrac{4\pi R k_B T N_A}{v_{solv}}\phi^2\left(\dfrac{1}{2} - \chi\right)\left(L - \dfrac{h}{2}\right)^2, for\ L < h < 2L \\ \dfrac{4\pi R k_B T N_A}{v_{solv}}\phi^2\left(\dfrac{1}{2} - \chi\right)\left\{L^2\left[\dfrac{h}{2L} - \dfrac{1}{4} - \ln\left(\dfrac{h}{L}\right)\right]\right\}, for\ h < L \end{cases} \tag{S3}$$

$$\Phi_{elas} = \frac{2\pi R k_B T {L_{ext}}^2 \phi \rho_{lig}}{MW_{lig}}\left\{\frac{h}{L_{ext}}\ln\left[\frac{h}{L_{ext}}\left(\frac{3 - h/L_{ext}}{2}\right)\right] - 6\ln\frac{3 - h/L_{ext}}{2} + 3\left(1 - \frac{h}{L_{ext}}\right)\right\}, for\ h < L_{ext} \tag{S4}$$

where A is the Hamaker constant between iron oxide NP cores, R is the NP radius, h is the NP surface-surface separation, k_B is Boltzmann constant, T is absolute temperature, N_A is Avogadro's constant, v_{solv} is the solvent molar volume, ϕ is ligand volume fraction in the ligand shell, χ is the Flory Huggins parameter, L is the effective ligand shell thickness, L_{ext} is the extended ligand shell thickness, ρ_{lig} is the density of oleic acid ligand,

and MW_{lig} is the molecular weight of ligand. Values of these parameters are listed in Table S2.

The total potential energy (Φ_{sum}) per NP is $\Phi_{sum} = 6 \times (\Phi_{VdW} + \Phi_{osm} + \Phi_{elas})$, in which VdW, osmotic and elastic potentials of one NP are shared by 12 nearest neighbors. VdW interactions between non-nearest neighbors are neglected.

We are not explicitly including ligand-ligand VdW attractions in the potential profile[3]. This is because we are treating the system at a constant pressure, where the attraction between ligands is always balanced by surrounding solvent molecules. For example, when the NP separation decreases, any VdW attraction increases between the ligands are balanced by decreases of attraction between solvent-ligand. In our system, at the SNSL growth stage, the solvent system is dominated by decane and dodecane, for which the attraction is similar between ligand-ligand and solvent-ligand. Therefore, no energy gain is achieved by replacing solvent with ligand, and the energy profile of carbon chain interactions remains unchanged.

Name	**Symbol**	**Value or Range**
Hamaker Constant	A	21 zJ
Temperature	T	298 K
Mole Volume of Solvent (Dodecane)	v_{solv}	2.2666×10^{-4} m^3/mol
Density of Ligand (Oleic Acid)	ρ	0.895×10^3 kg/m^3
Molecular Mass of Ligand (Oleic Acid)	MW_{lig}	4.692×10^{-25} kg
Ligand Shell Thickness in Solvent (Oleic Acid)	L_{ext}	1.8 nm
Effective Ligand Shell Thickness Solvated by Solvent Molecule	L	0 nm to 1.8 nm
Ligand Volume Fraction in the Ligand Shell	ϕ	50%
Flory–Huggins Interaction Parameter	χ	0

Table S2. Values of parameters used in the model.

References

1. Lu, C.; Akey, A. A.; Herman, I. P. *Appl. Phys. Lett.* **2012,** *101*, 133109.
2. Saunders, S. R.; Eden, M. R.; Roberts, C. B. *J. Phys. Chem. C* **2011,** *115*, 4603-4610.
3. Chen, Z. Y.; Moore, J.; Radtke, G.; Sirringhaus, H.; O'Brien, S. *J. Am. Chem. Soc.* **2007,** *129*, 15702-15709.